

Electronic Supplementary Information (ESI)

Carbon monoxide induced self-doping in methyammonium lead iodide films and associated long-term degradation effects

*Avi Mathur, Vivek Maheshwari**

Department of Chemistry, Waterloo Institute for Nanotechnology, University of Waterloo,

200 University Avenue West, Waterloo, Ontario N2L 3G1, Canada

E-mail: vmaheshw@uwaterloo.ca

Experimental Section

Synthesis of CH₃NH₃I precursor: Methylammonium iodide (MAI) was synthesized by dropwise addition of 30 mL of hydroiodic acid (57 wt. % in water, Sigma-Aldrich) to 27.8 mL of methylamine (33 wt. % in absolute ethanol, Sigma-Aldrich) under constant stirring at 0 °C. This solution was stirred for 2 hours and later, a dark yellow precipitate was recovered using a rotary evaporator at 60 °C for 1 hour. The solid precipitate was then washed and recrystallized with a copious amount of diethyl ether and ethanol, respectively, until it turned white. The resultant white precipitate was dried overnight to obtain the pure MAI.

Synthesis of perovskite precursor solution: The 1.35M perovskite solution was prepared by mixing 79.4 mg of MAI and 230.5 mg of lead iodide (99.999% trace metals basis, Sigma-Aldrich) in the solvent comprising 53.3 ul of dimethyl sulfoxide (anhydrous, ≥99.9%, Sigma-Aldrich) and 317.5 ul of N, N-dimethylformamide (anhydrous, 99.8%, Sigma-Aldrich). Further, 1 wt. % polystyrene (average Mw 35,000, Sigma-Aldrich) was added to the precursor solution to ensure resultant films stay stable and avoid moisture-induced degradation before exposure to carbon monoxide (CO). The solution was stirred on a magnetic stirrer for 30 minutes before spin-coating.

Spin coating of perovskite precursor solution and fabrication of perovskite-based photodetector: The perovskite films were spin-coated on Si/SiO₂ chips having equidistant gold electrodes at 200 μm to fabricate the lateral configuration of a self-powered photodetector device. The chips were initially washed with Millipore water and later ultrasonicated in acetone and isopropanol for 5 minutes each and finally, re-washed with Millipore water. The chips were then Piranha treated (3 H₂SO₄:1 H₂O₂) for 3 minutes, washed with copious Millipore water, and finally dried with an N₂ gun. The precursor perovskite solution was spin-coated on the cleaned chips at 4000 rpm for 30 seconds. Upon reaching 6 seconds of rotations, 200 μl of diethyl ether was added.

The obtained films were annealed stepwise at 65 °C for 2 minutes followed by 100 °C for 3 minutes to ensure complete perovskite phase formation.

Characterization

Structural, Microscopic, and Spectroscopic Characterization: The glancing incidence X-ray diffraction (GIXRD) patterns of obtained samples were measured using a PANalytical X'Pert Pro MRD diffractometer with Cu K α radiation ($\lambda = 1.54 \text{ \AA}$) at an incidence angle of 0.4°. The samples used for X-ray diffraction were exposed to a steady rate of dry air and CO under dark and light conditions, independently for 3 hours, and were not subjected to any external bias. A Zeiss Ultraplus field emission scanning electron microscopy (FE-SEM) equipped with energy-dispersive X-ray spectroscopy (EDX) was used to examine the surface topology and grain size distribution of the pristine and CO exposed perovskite films. Further, Raman spectroscopy was performed over Horiba HR800 spectrometer in the backscattering configuration. All Raman spectra were recorded at 532 nm excitation wavelength at a power of 6 mW. The samples used for FE-SEM and Raman spectroscopy consisted of perovskite films exposed to a steady flow of dry air and CO. This exposure to gases was either carried out in dark or under light for 60 minutes each. The poled perovskite films refer to the samples where a constant voltage of 2 V was applied across the gold electrode and ground, during the 60 minutes of exposure to requisite gases. The depth profile of freshly prepared and perovskite films exposed to CO for 6 hours was analyzed using time-of-flight ion mass spectroscopy by employing a Cs⁺ ion source (500 eV) for sputtering and Bi³⁺ (30 keV) for analysis over TOF-SIMS 5, ION-ToF GmbH. A Stanford Research Systems Universal Gas Analyzer (UGA) system was used to analyze the gases present in a custom-made sealed quartz beaker. The required gas was initially purged and maintained within the sealed beaker. Later, a 1.8 m long capillary tube (175 μm ID) was inserted in the beaker to monitor the

change observed in the partial pressures of O₂, N₂, and CO upon opening the outlet valve. The Young's Modulus maps were acquired using RTESPA 525 probes (Bruker) with a nominal spring constant of 200 N/m and resonant frequency of 525 kHz on a Bruker Dimension Icon in PeakForce QNM mode. The spring constant and deflection sensitivity of the probes were calibrated using a sapphire standard sample before each measuring session. The tip radius was estimated to be 20-30 nm, using a Titanium sample of known roughness. The elastic modulus for the sample surface was calculated following the Derjaguin-Muller-Toropov (DMT) model for tip-sample contact. The surface potential (V_{CPD}) maps were acquired with the topographic signal simultaneously at an effective tip-sample lift height of 80 nm on a Bruker Dimension Icon in Amplitude Modulated - Kelvin Potential Force Microscopy (AM-KPFM) mode using SCM PIT probe (Bruker). The topographic height was obtained by maintaining the amplitude of the first cantilever resonance at 65.8 kHz at a predefined amplitude setpoint of approximately 30 nm. The V_{CPD} was then determined by compensating the ac component of the electrostatic force at angular frequency ω with an applied dc voltage ($= |V_{\text{CPD}}|$) in a feedback control loop. To separate the topographic signal from the V_{CPD} signal, enhance the sensitivity and minimize the probe-sample convolution effects, the AC electrostatic force component was generated at the cantilever's 2nd resonance frequency of 411 kHz.

Electrical measurements: The electrical measurement on the planar lateral device configuration of the Au/MAPbI₃/Au self-powered photodetector was conducted using a probing station. A two-probe method was employed by connecting one probe to a gold electrode on the chip and another probe being connected to the ground. A Keysight 6614C 50-Watt system power supply with a maximum voltage output of 100 V was used for applying an external bias. For carrying out optoelectronic measurements of a perovskite-based self-powered photodetector device, an external

bias of 2 V was applied (referred to as poling) for 5 min underexposure of various gases (O₂, N₂, CO₂, and CO) and in ambient atmosphere. This poling time was chosen to induce optimum polarization in perovskite film without incurring spontaneous material degradation. Post poling, optoelectronic measurements including the open-circuit voltage (V_{oc}) and the short-circuit current (I_{sc}) were sequentially measured using a Keysight 3458A Digital multimeter. The film was connected in series with the multimeter and power supply to complete the circuit.

The illumination/light exposure, wherever reported, refers to simulated airmass 1.5 global irradiation (100 mW/cm²), generated using a Xenon-lamp based solar simulator (Newport Oriel Instrument 67005, 150 W Solar Simulator). An NREL calibrated KG5 silicon reference cell was used to calibrate light intensity to minimize any spectral mismatch.

Interpretation of work function from AM-KPFM

The KPFM measures the contact potential difference (V_{CPD}) between the conductive tip and the sample:

$$V_{CPD} = \frac{(\phi_{tip} - \phi_{sample})}{e}$$

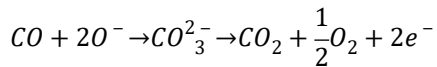
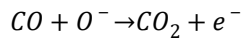
Where ϕ_{tip} and ϕ_{sample} represent the work function of the conductive tip and sample, respectively, and can be approximated as their respective Fermi level positions. A freshly cleaved highly oriented pyrolytic (HOPG) graphite with a stable work function (4.65 eV) was used as a reference sample to calibrate the work function of the KPFM probe. The absolute surface work function of the sample was then calculated by the following equation:

$$\phi_{sample} = 4.65 \text{ eV} + V_{CPD(HOPG)} - V_{CPD(sample)}$$

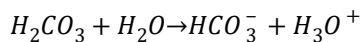
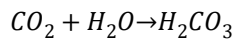
Further, to confirm the reliability of the technique in accurately determining the work function, a V_{CPD} map of a gold electrode patterned over a Si/SiO₂ wafer was acquired, as seen in Fig. S4. The calculated work function of gold (4.7 eV) matches well with the value reported in the literature for the gold surface exposed to ambient atmosphere.^{1, 2}

Potential Interaction Mechanism of CO and Perovskite

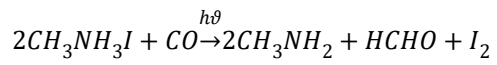
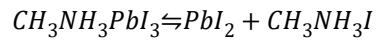
For perovskite film processed in an ambient atmosphere, molecular O₂ can dissociatively adsorb on the perovskite surface in form of reactive atomic oxygen species (O₂⁻, O[·] and O²⁻).³ We hypothesize that when such perovskite surface is exposed to CO, the reducing tendency of the CO allows it to react with pre-adsorbed reactive oxygen species leading to the formation of CO₂ by following reactions:^{4, 5}



Previous studies suggest that CO₂ and moisture can form carbonic acid and later lead to the formation of bicarbonate and hydronium ions on the perovskite surface. The bicarbonate and hydronium ion may replace the corresponding I⁻ and MA⁺ ions in the perovskite crystal structure leading to material degradation leaving behind PbI₂. The PbI₂ may form a stable complex of dicarboxyoxylead or Pb(HCO₃)₂.⁶ The presence of the PbI₂CO complex has also been reported in previous studies.⁷



Alternatively, under light, iodide ions in the perovskite may undergo an oxidation process⁸, with the released proton forming volatile formaldehyde as follows:



More detailed studies are required to ascertain the exact nature of the interaction between CO and MAPbI₃.

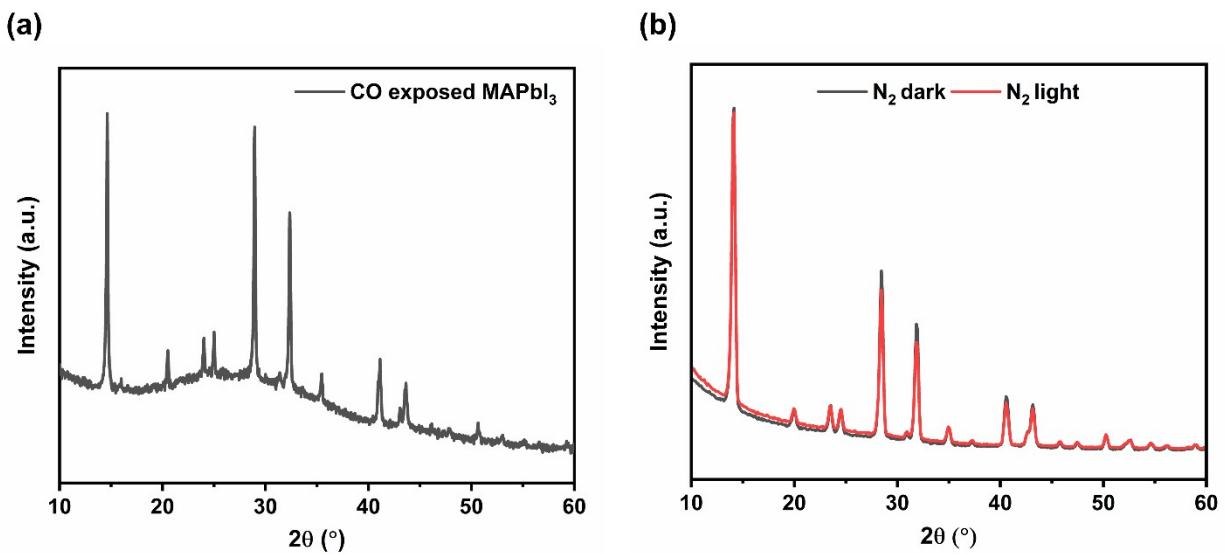


Fig. S1 (a) Powder XRD pattern of the MAPbI₃ film exposed to the CO environment confirming the absence of PbI₂ diffraction peak. Similarly, the PbI₂ impurity peak is not observed in the (b) GIXRD pattern of perovskite film stored in the N₂ atmosphere in dark and light.

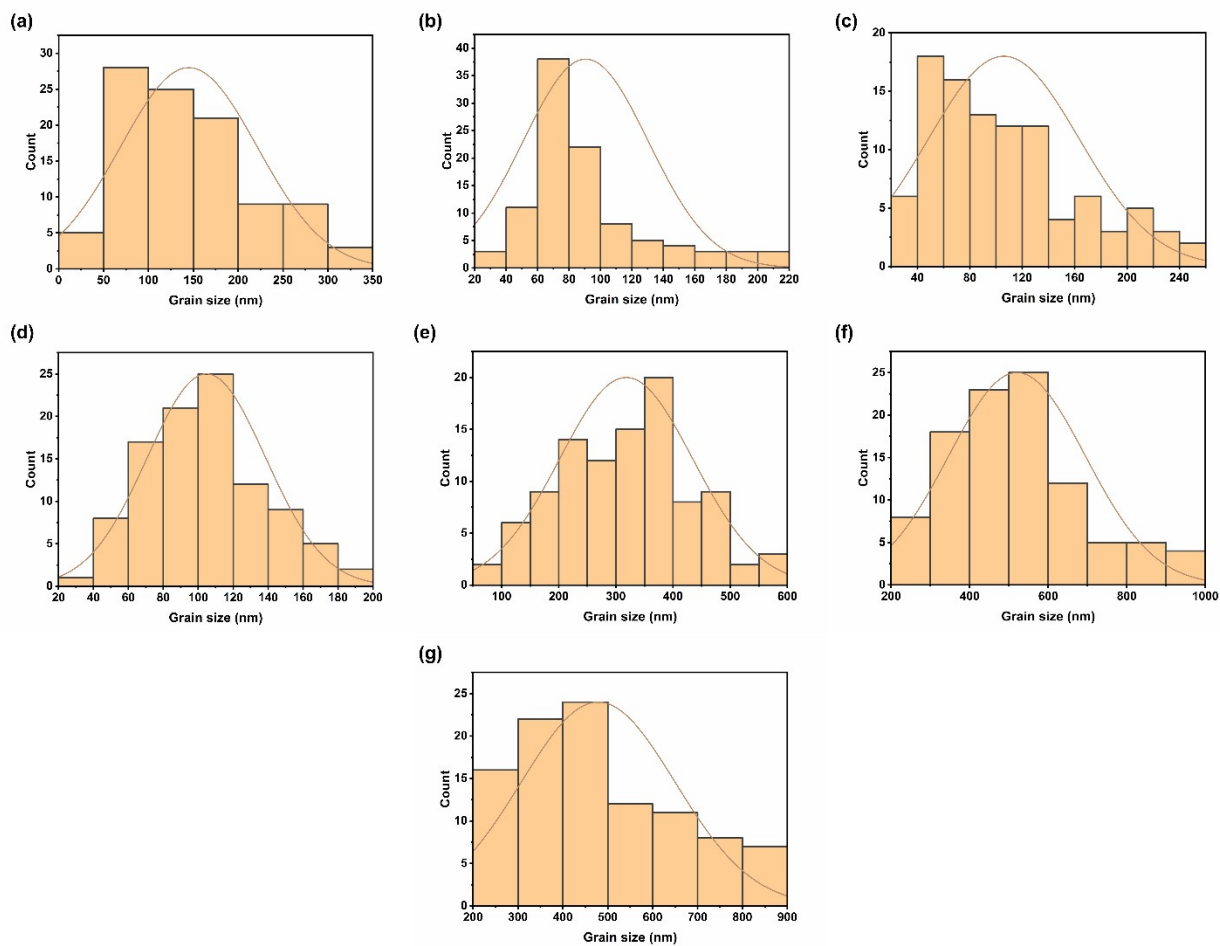


Fig. S2 Grain size distribution observed in (a) pristine perovskite film and MAPbI₃ film exposed to CO in dark for (b) 1-hour, (c) 3 hours, and (d) 1-hour with poling. Grain size distribution in perovskite film exposed to CO in light for (e) 1-hour, (f) 1-hour with poling, and (g) 3 hours.

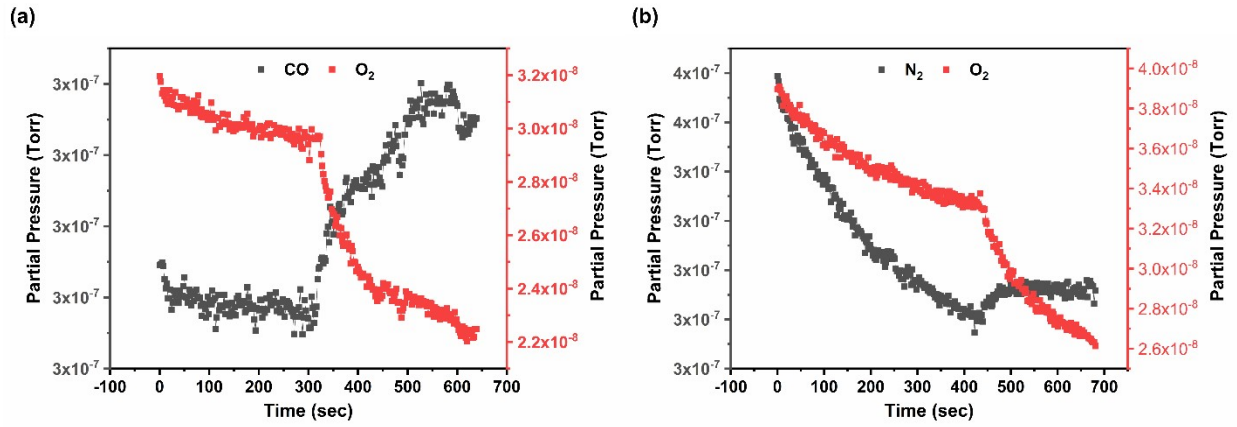


Fig. S3 Analysis of gases present in the sealed beaker where (a) a bare glass substrate is stored in CO atmosphere and (b) MAPbI₃ film is stored in N₂ atmosphere.

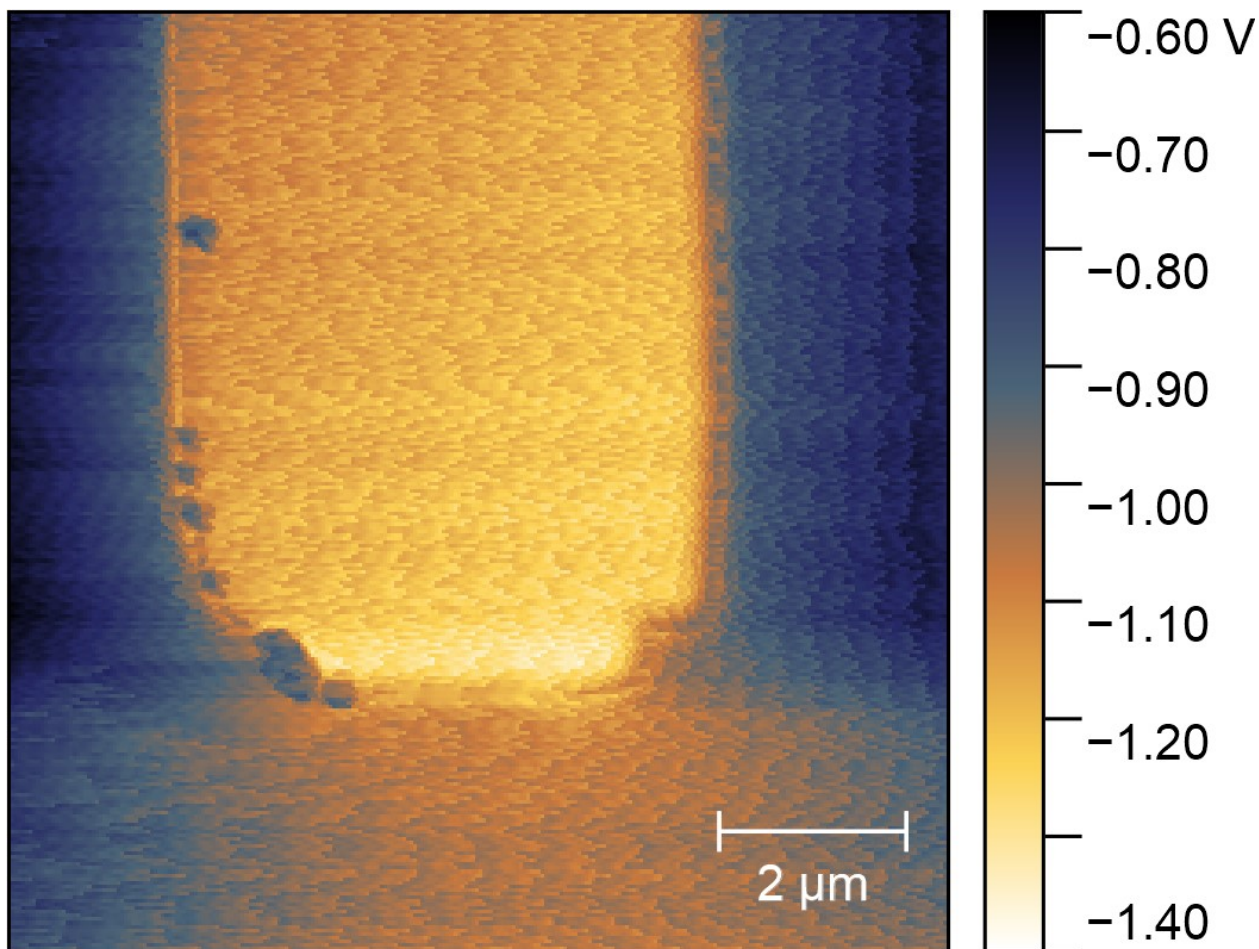


Fig. S4 Surface potential map of gold electrode patterned over a Si/SiO₂ wafer. The corresponding work function value is calculated to be 4.7 eV.

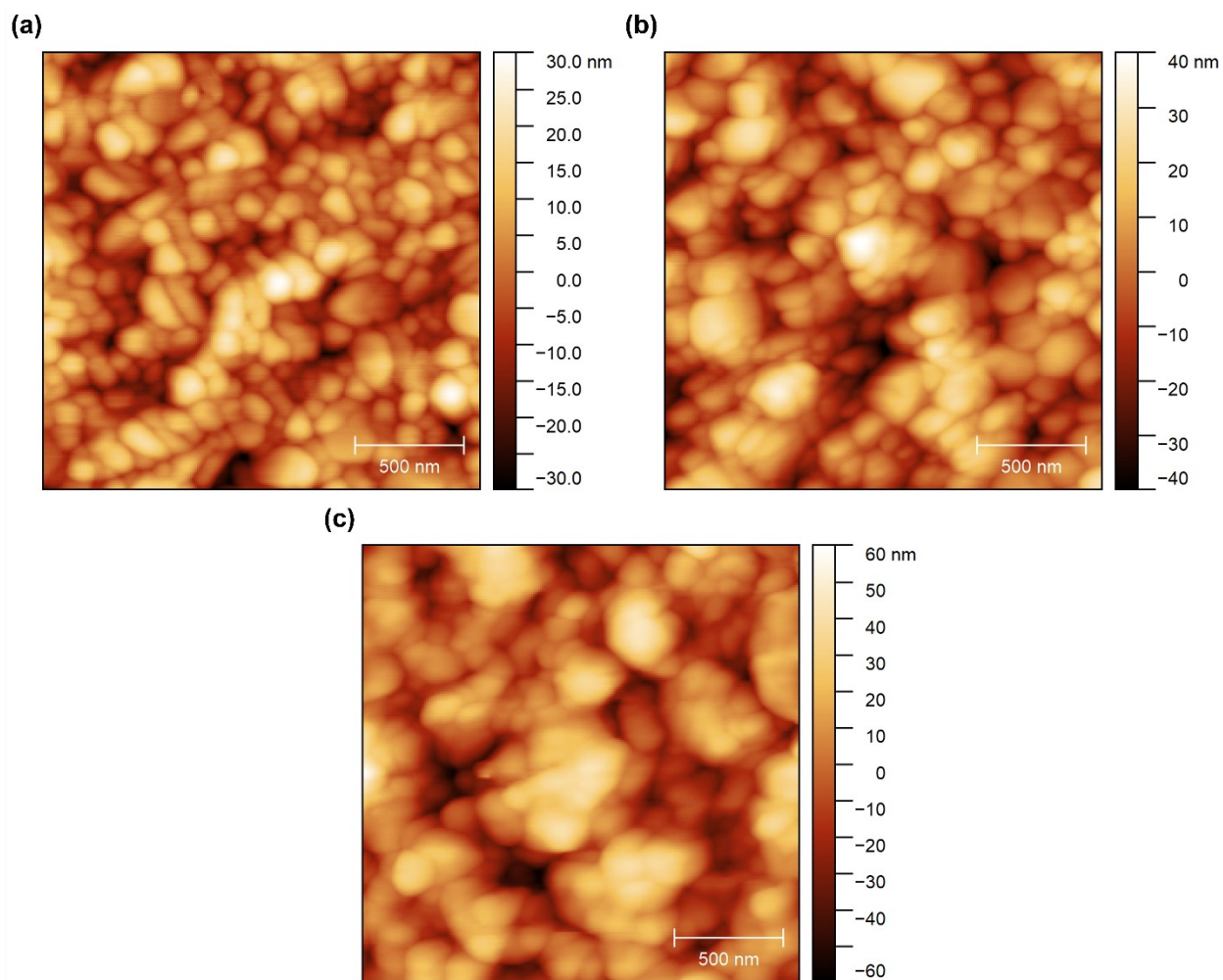


Fig. S5 AFM topography maps indicate an increase in surface roughness of the perovskite film over time when exposed to CO for (a) 0, (b) 6, and (c) 24 hours.

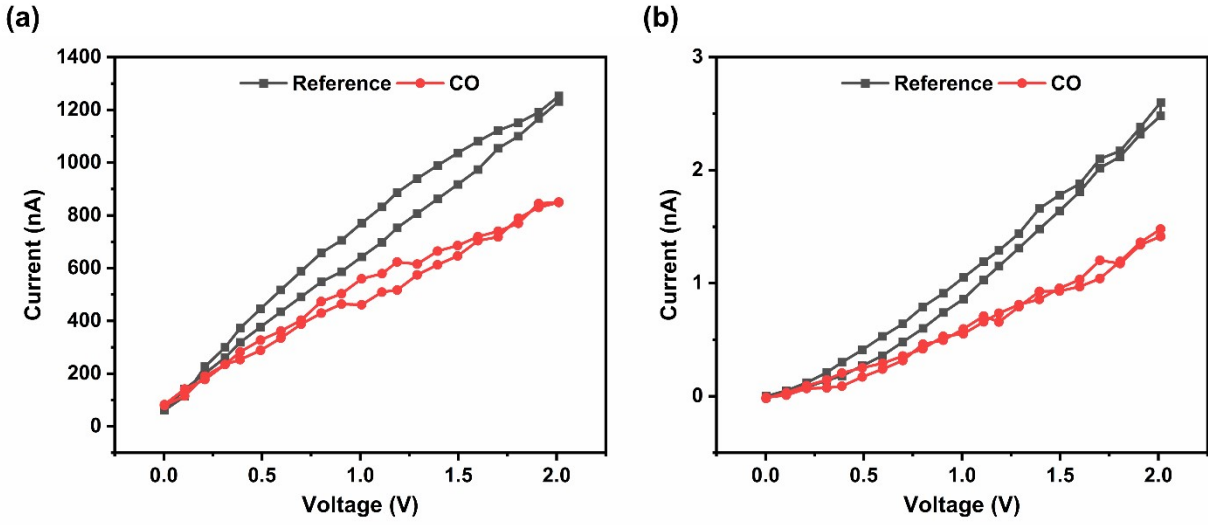


Fig. S6 *I-V* curves of perovskite films exposed to ambient (reference) and CO atmosphere under (a) 1.0 sun illumination and in (b) dark.

References

1. S. Rentenberger, A. Vollmer, E. Zojer, R. Schennach and N. Koch, *J. Appl. Phys.*, 2006, **100**, 053701.
2. W. N. Hansen and K. B. Johnson, *Surf. Sci.*, 1994, **316**, 373-382.
3. A. Salker, N.-J. Choi, J.-H. Kwak, B.-S. Joo and D.-D. Lee, *Sensors Actuators B: Chem.*, 2005, **106**, 461-467.
4. H.-J. Lin, J. P. Baltrus, H. Gao, Y. Ding, C.-Y. Nam, P. Ohodnicki and P.-X. Gao, *ACS Appl. Mater. Interfaces*, 2016, **8**, 8880-8887.
5. S. B. Karki, R. K. Hona and F. Ramezanipour, *J. Electron. Mater.*, 2020, **49**, 1557-1567.
6. M. Nayakasinghe, Y. Han, N. Sivapragasam, D. S. Kilin and U. Burghaus, *Chem. Commun.*, 2018, **54**, 9949-9952.
7. D. Tevault and K. Nakamoto, *Inorg. Chem.*, 1976, **15**, 1282-1287.
8. G. Abdelmageed, L. Jewell, K. Hellier, L. Seymour, B. Luo, F. Bridges, J. Z. Zhang and S. Carter, *Appl. Phys. Lett.*, 2016, **109**, 233905.